AUTOMOTIVE AIR CONDITIONING SYSTEM WITH AN INTERNAL HEAT EXCHANGER USING R1234YF AND DIFFERENT EVAPORATION AND CONDENSATION TEMPERATURES

by

Mehmet DIREK[a*] and Alper KELESOGLU[b]

[a] Department of Energy Systems Engineering, Yalova University, Yalova, Turkey
[b] Institute of Science and Engineering, Yalova University, Yalova, Turkey

Original scientific paper
https://doi.org/10.2298/TSCI170125215D

This study presents the energy and exergy analysis of a R1234yf automotive air conditioning system. For this aim, an experimental baseline automotive air conditioning system was developed and a double pipe internal heat exchanger was employed to the system. The detailed performance comparison of the system under different condensation and evaporation temperatures was studied for both the baseline system and the system with the internal heat exchanger. For this, the cooling capacity, COP, and the total exergy destruction per cooling capacity were evaluated. Additionally, the volumetric and isentropic efficiencies of the compressor were investigated. It was determined that the internal heat exchanger has increased COP and decreased exergy destruction per cooling capacity by 4%-6% and 13%-16%, respectively.

Key words: *R1234yf, internal heat exchanger, automotive air conditioning*

Introduction

One of the most important problems that humanity faces today is the growing greenhouse effect and global warming. Efforts to restrict the usage of chlorofluorocarbon, hydrochlorofluorocarbon, and hydrofluorocarbon (HFC) refrigerants, known to contribute to global warming, still continues. The R134a, with global warming potential (GWP) value of 1430, which belongs to the HFC group, is widely used in automotive air conditionig (AAC) systems. According to the EU Regulation No 517/2014, it is prohibited to use the refrigerants that has higher GWP than 150 from 2022 [1]. For that reason, the refrigerants that have low GWP values as an alternative to the R134a appeals significant attention for the automotive refrigeration applications. The literature related to these refrigerants shows that the R1234yf is seen as the most important alternative for the mobile climate control systems to protect the environment. The R1234yf has "0" ozone depletion potential value and GWP value below "4" without containing any chlorine in its chemical structure [2].

The R1234yf can be used directly or with small modifications instead of R134a in AAC systems [3]. However, recent studies showed that the cooling capacity and COP values were about 4% ~ 18% and 1% ~ 15% lower when R1234yf used is in the system designed for R134a without any modification [4-7]. This is due to the R1234yf has between 21% and 28% lower latent heat of vaporization at the same saturation temperature in comparison with R134a. To overcome this problem, sub-cooling temperatures can be increased by optimizing

* Corresponding author, e-mail: mehmetdirek@hotmail.com

the surface areas of the condenser and evaporator [8]. Zilio *et al.* [3] reported that the COP value of the system with R1234yf can exceed that of the system works with R134a when the evaporator and condenser surface areas enlarged by 20% and 10%, respectively. Furthermore, the cooling capacity can be increased by adding internal heat exchanger (IHX) between evaporator and condenser exits of the system [9]. Daviran *et al.* [10] developed a simulation program that can determine the performance parameters of the system components in the case of using R1234yf (2,3,3,3-tetrafluoropropene) as refrigerant in an AAC system that was designed for R134a. The results obtained with R1234yf show the decrease of both the total heat transfer coefficient and the pressure drop, respectively, by 18% ~ 21% and by 20% ~ 24% compared to results obtained with R134a. Qi [11] investigated the potentials for improving the system performance parameters for the operation of an automotive climate system with R1234yf as a refrigerant and determined experimental and comparative performance parameters with R134a. He found that the cooling capacity and COP values of the system were risen up to 15% by changing the sub-cooling degree from 1 K to 10 K in the condenser. Also, he claimed that the cooling capacity of the system can increase 72.8% by increasing the compressor volumetric efficiency from 55% to 95%. Moles *et al.* [12] made changes in the steam compression refrigeration system and compared the system performance parameters for R1234yf and R1234ze in different configurations. It is stated that the cooling capacity and COP values were increased when IHX was used in the system. Furthermore, when the effectiveness of the IHX for R1234yf exceeds 45%, they found that the COP value for the R1234yf was higher than that of R134a. Cho *et al.* [9] experimentally determined the performance of an automobile air conditioning system that designed for R134a without any change in the system for R1234yf. In addition, they tested the system to obtain the variation of the performance parameters by adding IHX for the R1234yf. In the absence of the IHX, they found that the cooling effect for R134a is less than that of R1234yf. However, they concluded that the cooling capacity of the R1234yf is 0.9% higher than that of R134a when the system with IHX exceeds 2500 rpm. Mota-Babiloni *et al.* [13] determined the performance parameters of an air conditioning system using R134a, R1234yf, and R1234ze experimentally and comparatively. The results for the three refrigerants are given as a function of different evaporator and condenser temperatures and comparatively. Compared to R134a, R1234yf, and R1234ze have lower cooling capacity values 9% and 30%, respectively. In addition, they claimed that the cooling capacity values were decreased for the increased condensation temperatures from 313.15 K to 333.15 K. They concluded that the cooling capacity and COP of the system with R1234yf would tend to increase by adding IHX at 30% effectiveness. Navarro-Esbri *et al.* [14] tested the performance of R1234yf as an alternative refrigerant in a refrigeration cycle that uses R134a. In case of using R1234yf, they experimentally analysed the effect of IHX on the performance parameters of the system and the results were given comparatively between two refrigerants. As a result, it is stated that the cooling capacity of the system is improved by 6% when IHX is used with the R1234yf.

In this study the experimental AAC system which designed for R134a were established and the low GWP refrigerant R1234yf were adapted directly to the system. Furthermore, the effect of IHX was investigated under different evaporation and condensation temperature for the refrigerant R1234yf. In order to determine the performance of the system with/without IHX, a non-dimensional number was evaluated as a ratio between total exergy destruction and cooling capacity. The volumetric and isentropic efficiencies of the compressor were also evaluated for different operating conditions and the results were discussed.

Description of the experimental set-up

The experiments were conducted in a conventional mechanical compression refrigeration system that uses R134a in automobiles. These components are a belt-driven compressor, a parallel flow condenser, a laminar microchannel evaporator, a thermostatic expansion valve (TXV), a liquid tank, a filter, and a dryer, as seen in fig. 1. The characteristics of the experimental system components were given in tab. 1. The evaporator and the condenser were located at the exit cross-sections of the two separate 1 m air ducts. Furthermore, a 900 mm length double-pipe heat exchanger was connected to the evaporator and condenser outlets. Additionally, two individual electric heaters were employed in the evaporator and condenser duct to provide the desired air-flow temperature. For this purpose, a 5 kW electric heater was mounted at about 25 cm from the condenser fan at the condenser air duct and a 2 kW electric heater was mounted about 20 cm from the evaporator fan at the evaporator air duct. The cross-sections of evaporator and condenser air ducts are 0.24 m × 0.24 m and 0.67 m × 0.35 m, respectively. In order to provide the desired air-flow in these ducts, radial fans were installed at each duct. The vapour line diameter is 5/8“ and the liquid line diameter is 3/8“ within the tubing. Also, the tubing was insulated with the elastomeric insulation material that is suitable for their diameters.

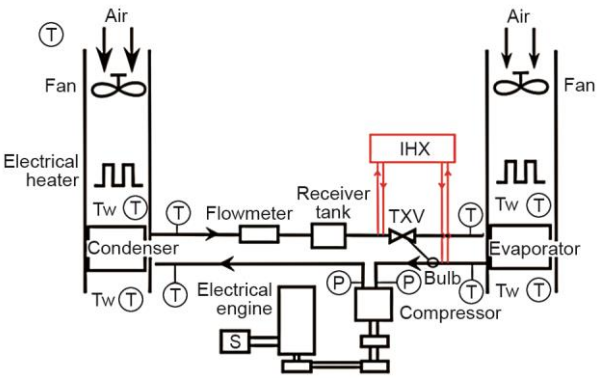

Figure 1. Schematic diagram of the experimental system

The temperature of the refrigerant at various points in the experimental system were measured with K-type (NiCr-Ni) thermocouples. The measured temperatures were recorded on a computer *via* temperature measurement data collection system. The volume flow rate of the refrigerant was measured by a turbine type volume flow meter which was connected to the liquid line. In addition, the vaporization and condensation pressures of the refrigerant were measured by a digital manifold. Table 2 shows the range and uncertainty of the measuring devices.

Table 1. Specifications of equipment of AAC system

Component	Specification
Compressor	Stroke volume: 138 cm^3 Cylinder numbers: 7 Max. speed: 5000 rpm
Condenser	Capacity: 5.34 kW Dimensions: 635 mm × 355 mm × 20 mm Number of channels: 31
Evaporator	Capacity: 5.23 kW Dimensions: 210 mm × 275 mm × 70 mm Number of channels: 20

Table 2. Specifications of the instrumentation

Measured variable	Instrument	Range	Uncertainty
Temperature	K-type thermocouple	–300-500 ºC	±0.5%
Pressure	Digital manifold	0-40 bar	±0.75%
Air velocity	Anemometer	0.1-20 m/s	±2%
Volume flow rate	Turbine flow meter	0.2-1.2 m^3/h	±1%

Testing procedure

In the experiments, air was supplied with 0.5 m^3/s volumetric flow rate to the condenser duct. In addition, the fan connected to the evaporator duct was operated at maximum speed and the volumetric flow rate of the air was set to 0.15 m^3/s. Also, a 1000 g refrigerant R1234yf was charged from the manifold to the system. The system was tested with two different approaches. First, the evaporation temperatures was changed from –5 °C to –20 °C with 5 °C temperature increments where the condensation temperature was constant at 40 °C. Secondly, the condensation temperatures was changed from 40 °C to 50 °C with 2 °C temperature increments where the evaporation temperature was constant at –10 °C. These evaporation and condensation temperature changes were done by arranging the optimum inlet air temperature by regulating the current characteristics of the each evaporator and condenser duct heater.

Thermodynamic analysis

Energy analysis was done by applying the First law of thermodynamics to the each component of the AAC system. The exergy analysis was performed under Second law of thermodynamics. The reference states were taken as $T_0 = 25\,[^\circ\mathrm{C}]$. Accordingly, the energy analysis for a steady-state system can be evaluated by:

$$\dot{Q}_{\mathrm{CV}} - \dot{W}_{\mathrm{CV}} = \sum \dot{m}_{\mathrm{i}} h_{\mathrm{i}} - \sum \dot{m}_{\mathrm{o}} h_{\mathrm{o}} \tag{1}$$

Also the exergy analysis for a steady-state system was calculated by:

$$\dot{E}x_{\mathrm{d}} = \sum \left(1 - \frac{T_0}{T}\right)\dot{Q} - \sum \dot{W} + \sum_{\mathrm{i}} \dot{m}\psi - \sum_{\mathrm{o}} \dot{m}\psi \tag{2}$$

$$\psi = (h - h_0) - T_0(s - s_0) \tag{3}$$

Assuming no heat loss from the compressor, the energy and exergy values can be obtained using:

$$\dot{W}_{\mathrm{comp}} = \dot{m}_{\mathrm{r}}\left(h_2 - h_1\right) \tag{4}$$

$$\dot{E}x_{\mathrm{d,comp}} = \dot{m}_{\mathrm{r}}(\psi_1 - \psi_2) + \dot{W}_{\mathrm{comp}} \tag{5}$$

Also, assuming no heat loss from the expansion valve, the enthalpy values of the inlet and exit stream of refrigerant is equal and the exergy destruction can be found from:

$$h_3 = h_4 \tag{6}$$

$$\dot{E}x_{\mathrm{d,TXV}} = \dot{m}_{\mathrm{r}}(\psi_3 - \psi_4) = \dot{m}_{\mathrm{r}} T_0 (s_4 - s_3) \tag{7}$$

The energy and exergy analysis of the evaporator and condenser can be expressed:

$$\dot{Q}_{\text{evap}} = \dot{m}_{\text{r}}(h_4 - h_1) \tag{8}$$

$$\dot{E}x_{\text{d,evap}} = \dot{m}_{\text{r}}(\psi_1 - \psi_4) + \dot{Q}\left(1 - \frac{T_0}{T_{\text{evap}}}\right) \tag{9}$$

$$\dot{Q}_{\text{cond}} = \dot{m}_{\text{r}}(h_3 - h_2) \tag{10}$$

$$\dot{E}x_{\text{d,cond}} = \dot{m}_{\text{r}}\left[(h_2 - h_3) - T_0(s_2 - s_3)\right] - \dot{Q}\left(1 - \frac{T_0}{T_{\text{cond}}}\right) \tag{11}$$

The energy and exergy destruction for the IHX can be determined from:

$$h_{\text{i},1} + h_{\text{i},3} = h_{\text{o},2} + h_{\text{o},4} \tag{12}$$

$$\dot{E}x_{\text{d,IHX}} = \dot{m}_{\text{r}}(\psi_{\text{i,evap}} - \psi_{\text{o,evap}}) + \dot{m}_{\text{r}}(\psi_{\text{i,cond}} + \psi_{\text{o,cond}}) \tag{13}$$

The COP of the AAC system can be obtained from:

$$COP = \frac{\dot{Q}_{\text{evap}}}{\dot{W}_{\text{comp}}} \tag{14}$$

The total exergy destruction for the AAC system can be obtained from:

$$\dot{E}_{\text{d}} = \dot{E}x_{\text{d,comp}} + \dot{E}x_{\text{d,cond}} + \dot{E}x_{\text{d,TXV}} + \dot{E}x_{\text{d,evap}} + \dot{E}x_{\text{d,IHX}} \tag{15}$$

The volumetric efficiency and isentropic efficiency of the compressor could be found from:

$$\dot{m}_{\text{ref}} = \frac{\rho_{\text{suc}} V_G N}{60} \tag{16}$$

$$\eta_{\text{vol}} = \frac{\dot{m}_{\text{ref}}}{\dot{m}_r} \tag{17}$$

$$\eta_{\text{isen}} = \frac{h_{2s} - h_1}{h_2 - h_1} \tag{18}$$

In this paper, only the refrigerant was replaced for the same experimental system which designed for R134a, thus the results strongly depend on the specifications of the equipment. Therefore, to overcome this relevance, a non-dimensional comparison parameter $\dot{E}_{\text{d}}/\dot{Q}_{\text{evap}}$ was introduced.

Results and discussion

In this section the results obtained from the energy and exergy analysis were discussed under two different topics relevant to the operating temperatures of evaporator and condenser. The COP, cooling capacity, volumetric efficiency, isentropic efficiency, and the

total exergy destruction per cooling capacity values were analysed. Using the RSS method, the calculated uncertainity values for the performance parameters are ±0.88%, ±0.71%, ±1.18%, ±1.68%, ±1.76%, respectively [15].

The results under constant evaporation temperature

Figure 2(a) shows the change in cooling capacity while the evaporation temperature kept constant at –10 °C with the variable condensation temperatures from 40 °C to 50 °C. The cooling capacity at 40 °C condensation temperature without IHX was calculated as 3.89 kW. When the condensation temperature rises up to 50 °C, the cooling capacity decreased to 3.47 kW. The main reason for the decrease is the decrease in the rejection of heat from the condenser and the transfer of heat from the air stream passing through the evaporator duct due to the increase in the condensation temperature. When the IHX was adapted to the system, it was observed that the systems cooling capacity had increased meanly by 11% due to the increased enthalpy difference with the increasing sub-cooling degree. Figure 2(b) shows the change in COP value depending on the condensation temperature. As a result of the increased condensation temperature, the compressor power increased and the cooling capacity decreased and this results in the dropped COP. When the IHX employed to the system, the COP value increased due to higher increasing rate for cooling capacity in comparison with compressor power. For instance, the COP value at the 44 °C condensation temperature without IHX was calculated as 3.73, while under the same conditions with the IHX it was calculated as 3.93. Figure 2(c) shows the change of the compressor power with respect to the condensation temperature. While the condensation temperature increases, the condensation pressure increases and accordingly the compressor power increases. This is also the main reason for the decline in COP. From fig. 2(d), it can be seen the TXV inlet temperature increased when the condensation temperature increased. This is due to the increase in condensation pressure with increasing condensation temperature and the increase in the outlet temperatures of the refrig-

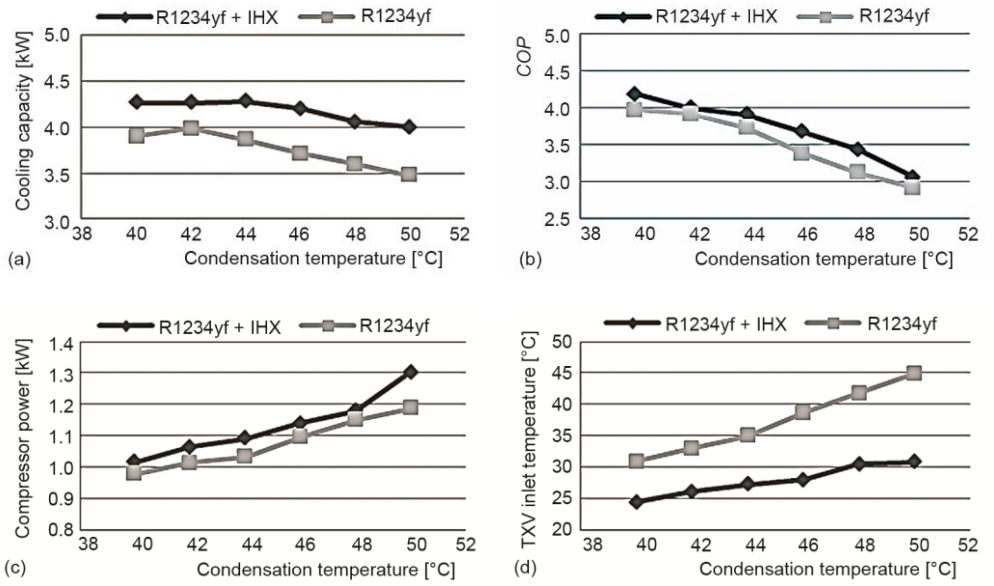

Figure 2. (a) Cooling capacity, (b) COP, (c) compressor power, (d) TXV inlet temperature

erant from the evaporator. However, with addition of the IHX, the sub-cooling degree of the system increased and the TXV inlet temperature decreased at the same evaporation temperature. For instance, at 40 °C condensation temperature without IHX, the TXV inlet temperature was measured 32 °C. However, it was reduced 7 °C due to the higher sub-cooling degree by adding IHX and it was measured as 25 °C.

When the temperature of the air at the inlet of the condenser duct increases, the temperature of the refrigerant passing through the condenser increases, and accordingly, the temperature of the refrigerant passing through the system increases. This temperature increment for the refrigerant at the outlet of the condenser would increase the temperature at the outlet of evaporator due to IHX, and then it increases compressor working temperature and thus the volumetric efficiency of the system. This phenomenon can be shown in fig. 3(a). Unlikely, the isentropic compressor efficiency yields to decrease due to the increasing irreversibities, thus the entropy values as seen in fig. 3(b).

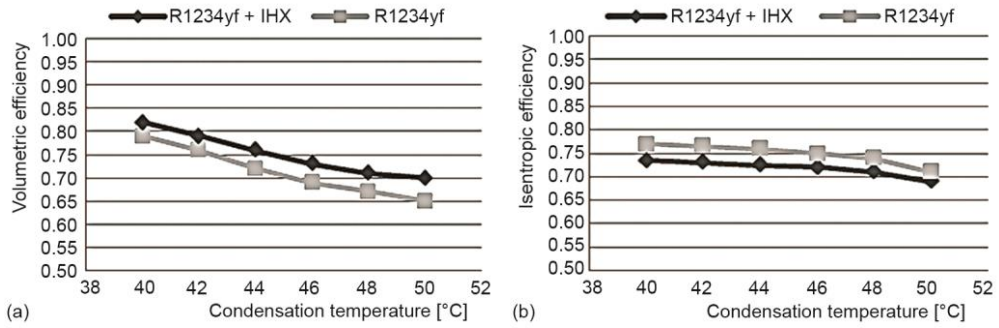

Figure 3. (a) Change in volumetric efficiency, (b) change in isentropic efficiency

The results under constant condensation temperature

The cooling capacity and the COP values of the experimental system were calculated where the condensation temperature is 40 °C and the evaporation temperature varies from –20 °C to –5 °C. The cooling capacity was increased due to the diminished temperature difference between the air-flow at the evaporator duct and the refrigerant by the raise of evaporation temperature as seen in fig. 4(a). As shown in figs. 4(b) and 4(c), when the evaporation temperature increases, the compressor power tends to decrease and this leads to an increase in the COP with the increase in cooling capacity. When the IHX employed to the system, the cooling capacity increases and the compressor power decreases due to the increasing sub-cooling degree and compressor suction temperature. This effect is very similar to the effect of increased evaporation temperature on COP. But for the constant condensation temperature, IHX has less sensible effect on the compressor power when the evaporation temperature increases for the system in comparison with constant evaporation temperature findings because of the temperature difference between the inlet and outlet of the compressor. In addition, the cooling capacity tends to increase due to the raise of the latent heat of vaporization with regard to the increasing evaporation temperature. Furthermore, the TXV inlet temperature increases with the increasing evaporation temperature. This has inverse effect with the constant evaporation temperature but less sensible. On the other hand, the TXV inlet temperature reduced by adding IHX to the system as shown in fig. 4(d). This temperature drop helps to prevent flash gas formation at the inlet of TXV.

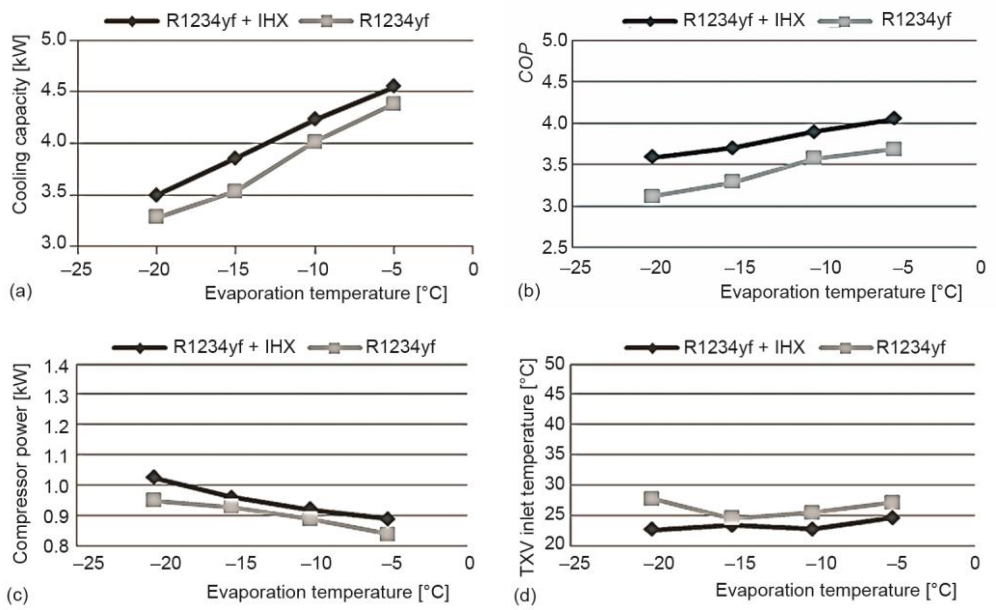

Figure 4. (a) Cooling capacity, (b) COP, (c) compressor power, (d) TXV inlet temperature

The density of refrigerant at the suction side of the compressor decreases with increasing evaporation temperature. This causes a reduction in the theoretical mass-flow rate against the measured mass-flow rate. Thus the volumetric efficiency of the AAC system increases. The IHX reduces the evaporator inlet temperature, thus the suction temperature at the inlet of the compressor. This results in an opposite effect on the volumetric efficiency as seen in fig. 5(a). The isentropic efficiency decreases with increasing evaporation temperature due to the raise in entropy values. The inverse IHX effect on the volumetric efficiency is valid for isentropic efficiency as shown in fig. 5(b).

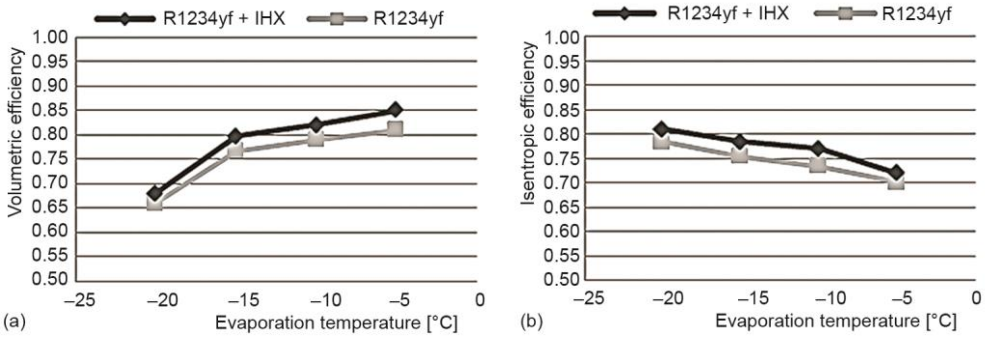

Figure 5. (a) Change in volumetric efficiency, (b) change in isentropic efficiency

Total exergy analysis of the system

The non-dimensional comparison parameter $\dot{E}_{\mathrm{d}}/\dot{Q}_{\mathrm{evap}}$ shows the effect of IHX clearly because it is independent from the configuration of the experimental system. From

this, evaluating this parameter regarding to the different condensation and evaporation temperatures allow us to seek the system performance for different operation conditions. With increasing condensation temperature at fixed air temperature in the condenser duct, the temperature difference increases between the refrigerant and the air stream, so that the exergy destruction was increased for the condenser. Along with that, the exergy destruction for the compressor, evaporator and TXV would increase due to the increased refrigerant temperature in the system. These changes cause an increase in the total exergy destruction while the cooling capacity of the system decreases. As a result the $\dot{E}_{\mathrm{d}}/\dot{Q}_{\mathrm{evap}}$ ratio is increasing as shown in fig. 6(a). On the other hand, the reverse effects were obtained for the components with increasing evaporation temperature. Furthermore, the rate of increase for the cooling capacity is higher than the total exergy destruction considering the increasing evaporation temperature. Figure 6(b) shows this behaviour for the system.

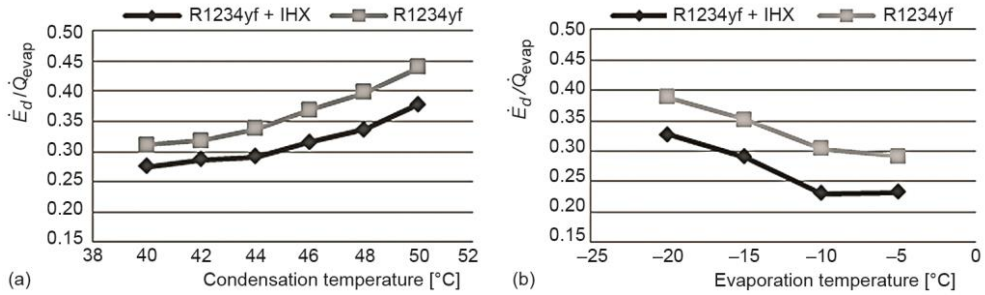

Figure 6. Exergy destruction per cooling capacity for (a) variable condensation temperature, (b) variable evaporation temperature

The usage of IHX reduces the temperature of the refrigerant at the inlet of the TXV and thus the exergy destruction rate. On the other hand, the exergy destruction for the condenser was increased due to the increased the subcooling degree. Additionally, it increased volumetric and isentropic efficiency of the compressor and yields to a reduction in $\dot{E}_{\mathrm{d}}/\dot{Q}_{\mathrm{evap}}$. On the contrary, the cooling capacity of the system increases as explained before. As a result of these effects of IHX, the $\dot{E}_{\mathrm{d}}/\dot{Q}_{\mathrm{evap}}$ values are lower than the configuration of the system without IHX.

Conclusions

The scope of the study was to determine the effect of IHX on the experimental AAC system with R1234yf. For this reason, double pipe heat exchanger was selected and experimental analysis was performed. Based on experimental data, cooling capacity, COP, and the total exergy destruction per cooling capacity were determined and presented as a function of constant evaporation or condensation temperatures. For both cases with IHX the results obtained from the calculations can be expressed as follows.

- Cooling capacity was increased meanly 11% ~ 12%.
- The COP value was improved about 4% ~ 6%.
- Compressor power was increased between 5% ~ 8%.
- Volumetric efficiency value was increased about 4% ~ 5%.
- Isentropic efficiency value was increased about 3% ~ 4%.
- Total exergy destruction per cooling capacity value was decreased meanly 13% ~ 16%.

Finally, after all aforementioned analysis, we can conclude that higher cooling capacity and COP can be achieved by using IHX for the AAC system working with R1234yf.

Nomenclature

$\dot{E}x$ – exergy destruction, [W]
h – enthalpy, [kJkg^{-1}]
$\dot{m}$ – mass flow rate, [kgs^{-1}]
N – rotational speed, [rpm]
s – entropy, [kJkg^{-1}K^{-1}]
T – temperature, [°C]
$\dot{Q}$ – heat transfer rate, [W]
$\dot{V}$ – volume, [m^3]
$\dot{W}$ – power, [W]

Greek symbols

ψ – flow specific exergy [Jkg^{-1}]
ρ – density, [kgm^{-3}]
η – efficiency, [%]

Subscripts

CV – control volume
i – inlet
o – outlet
d – destruction
comp – compressor
cond – condenser
evap – evaporator
r – refrigerant
TXV – thermostatic expansion valve
0 – dead state
IHX – internal heat exchanger
ref – reference
suc – suction
G – geometric
v – volumetric
isen – isentropic
w – wet

Acknowledgments

The authors would like to thank the University of Yalova for supporting this study through a Research Project No: 2015/BAP/123.

References

[1] ***, Regulation (Eu) No 517/2014 of The European Parliament And of the Council of 16 April 2014 on „Fluorinated Greenhouse Gases and Repealing Regulation EC No:842/2006”
[2] Papadimitriou, V. C., *et al.*, CF3CF=CH2 and (Z)-CF3CF=CHF: Temperature Dependent OH Rate Coefficients and Global Warming Potentials, *The Journal of Physical Chemistry*, *10* (2008), 6, pp. 808-820
[3] Zilio, C., *et al.*, The Refrigerant R1234yf in Air Conditioning Systems, *Energy*, *36* (2011), 10, pp. 6110-6120
[4] Wang, C. C., System Performance of R-1234yf Refrigerant in Air-Conditioning and Heat Pump System – an Overview of Current Status, *Applied Thermal Engineering, 73* (2014), 2, pp. 1412-1420
[5] Direk, M., *et al.*, Comparative Performance Analysis of Experimental Frigorific Air Conditioning System Using R-134a and Hfo-1234yf as a Refrigerant, *Thermal Science*, *20* (2016), 6, pp. 2065-2072
[6] Lee, T., *et al.*, Development of Performance Analysis Program and the Study of Substitution Refrigerant R1234yf for Vehicle Refrigerant Compressor, *Korean Journal of Air-Conditioning Refrigeration Engineering*, *23* (2011), 11, pp. 699-704
[7] Leck, T. J., Evaluation of R1234yf as a Potential Replacement for R-134a in Refrigeration Applications, *Proceedings*, 3rd IIR Conference on Thermo-Physical Properties and Transfer Processes of Refrigerants, Boulder, Col., USA, 2009, pp. 1-9
[8] Petitjean, S., *et al.*, R-1234yf Validation & A/C System Energy Efficiency Improvements, *Proceedings*, SAE Alternate Refrigerant Symposium, Scottsdale, Ariz., USA, 2010
[9] Cho, H., *et al.*, Exprimental Investigation of Performance and Exergy Analysis of Automotive Air Conditioning Systems Using Refrigerant R1234yf at Various Compressor Speeds, *Applied Thermal Engineering, 101* (2016), May, pp. 30-37
[10] Daviran, S., *et al.*, A Comparative Study on the Performance of R1234yf and HFC-134a as an Alternative in Automotive Air Conditioning Systems, *Applied Thermal Engineering, 110* (2017), Jan., pp. 1091-1100
[11] Qi, Z., Performance Improvement Potentials of R1234yf Mobile Air Conditioning System, *International Journal of Refrigeration*, *58* (2015), Oct., pp. 35-40

[12] Moles, F., *et al.*, Theoretical Energy Performance Evaluation of Different Single Stage Vapour Compression Refrigeration Configurations Using R1234yf and R1234ze(E) as Working Fluids, *International Journal of Refrigeration*, *44* (2014), Aug., pp. 141-150
[13] Mota-Babiloni, A., *et al.*, Drop-in Energy Performance Evaluation of R1234yf and R1234ze (E) in A Vapor Compression System as R134a Replacements, *Applied Thermal Engineering, 71* (2014), 1, pp. 259-265
[14] Navarro-Esbrí, J., *et al.*, Experimental Analysis of R1234yf as a Drop-in Replacement for R134a in a Vapor Compression System, *International Journal of Refrigeration, 36* (2013), 3, pp. 870-880
[15] Taylor, J. R., *An Introduction to Error Analysis Second ed.*, University Science Books, Sausalito, Cal., USA, 1997

Paper submitted: January 25, 2017
Paper revised: October 25, 2017
Paper accepted: October 28, 2017